Ultra-high-temperature ceramics

Ultra-high-temperature ceramics (**UHTCs**) are a class of refractory ceramics that offer excellent stability at temperatures exceeding 2000 °C[1] being investigated as possible thermal protection system (TPS) materials, coatings for materials subjected to high temperatures, and bulk materials for heating elements. Broadly speaking, UHTCs are borides, carbides, nitrides, and oxides of early transition metals. Current efforts have focused on heavy, early transition metal borides such as hafnium diboride (HfB_2) and zirconium diboride (ZrB_2);[2][3] additional UHTCs under investigation for TPS applications include hafnium nitride (HfN),[4] zirconium nitride (ZrN),[5] titanium carbide (TiC),[6] titanium nitride (TiN), thorium dioxide (ThO_2),[7][8] tantalum carbide (TaC)[9] and their associated composites.[10]

History

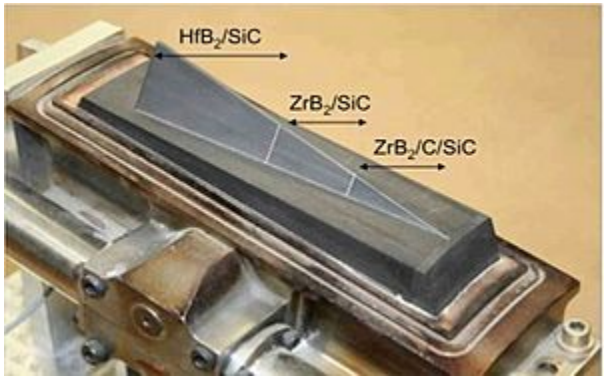

Figure 1. An UHTC strake composed of three different sections with different UHTC compositions.[11]

Beginning in the early 1960s, demand for high-temperature materials by the nascent aerospace industry prompted the US Air Force Materials Laboratory to begin funding the development of a new class of materials that could withstand the environment of proposed hypersonic vehicles such as the Boeing X-20 Dyna-Soar and the Space Shuttle at Manlabs Incorporated. Through a systematic investigation of the refractory properties of binary ceramics, they discovered that the early transition metal borides, carbides, and nitrides had surprisingly high thermal conductivity, resistance to oxidation, and reasonable mechanical strength when small grain sizes were used. Of these, ZrB_2 and HfB_2 in composites containing approximately 20% volume SiC were found to be the best performing.[12]

UHTC research was largely abandoned after the pioneering mid-century Manlabs work due to the completion of the Space Shuttle missions and the elimination of the Air force spaceplane development. Three decades later, however, research interest was rekindled by a string of 1990s era NASA programs aimed at developing a fully reusable hypersonic spaceplane such as the National Aerospace Plane, Venturestar/X-33, Boeing X-37, and the Air Force's Blackstar program.[13] New research in UHTCs was led by NASA Ames, with research at the center continuing to the present through funding from the NASA Fundamental Aeronautics Program. UHTCs also saw expanded use in varied environments, from nuclear engineering to aluminum production.

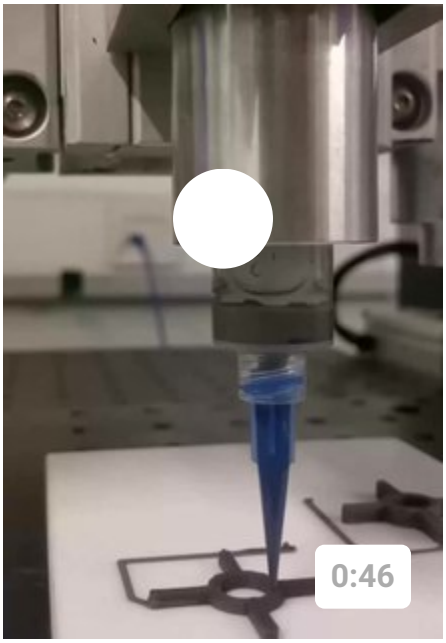

Production of a hafnium diboride set of fins via robocasting, a 3D Printing technique. 0.41mm nozzle, 4x speed.

In order to test real world performance of UHTC materials in reentry environments, NASA Ames conducted two flight experiments in 1997 and 2000. The slender Hypersonic Aero-thermodynamic Research Probes (SHARP B1 and B2) briefly exposed the UHTC materials to actual reentry environments by mounting them on modified nuclear ordnance Mk12A reentry vehicles and launching them on Minuteman III ICBMs. Sharp B-1 had a HfB2/SiC nosecone with a tip radius of 3.5 mm which experienced temperatures well above 2815 °C during reentry, ablating away at an airspeed of 6.9 km/s as predicted; however, it was not recovered and its axially-symmetric cone shape did not provide flexural strength data needed to evaluate the performance of UHTCs in linear leading edges.[14] To improve the characterization of UHTC mechanical strength and better study their performance, SHARP-B2, was recovered and included four retractable, sharp wedge-like protrusions called "strakes" which each contained three different UHTC compositions which were extended into the reentry flow at different altitudes.

The SHARP-B2 test that followed permitted recovery of four segmented strakes which had three sections, each consisting of a different HfB_2 or ZrB_2 composite as shown in Figure 1.[11] The vehicle was successfully recovered, despite the fact that it impacted the sea at three times the predicted velocity. The four rear strake segments (HfB_2) fractured between 14 and 19 seconds into reentry, two mid segments (ZrB_2/SiC) fractured, and no fore strake segments (ZrB_2/SiC/C) failed.[11] The actual heat flux was 60% less than expected, actual temperatures were much lower than expected, and heat flux on the rear strakes was much higher than expected. The

material failures were found to result from very large grain sizes in the composites and pure ceramics, with cracks following macroscopic crystal grain boundaries. Since this test, NASA Ames has continued refining production techniques for UHTC synthesis and performing basic research on UHTCs.[15]

Physical properties

Most research conducted in the last two decades has focused on improving the performance of the two most promising compounds developed by Manlabs, ZrB_2 and HfB_2, though significant work has continued in characterizing the nitrides, oxides, and carbides of the group four and five elements.[16][17][18][19] In comparison to carbides and nitrides, the diborides tend to have higher thermal conductivity but lower melting points, a tradeoff which gives them good thermal shock resistance and makes them ideal for many high-temperature thermal applications. The melting points of many UHTCs are shown in Table 1.[11] Despite the high melting points of pure UHTCs, they are unsuitable for many refractory applications because of their high susceptibility to oxidation at elevated temperatures.

Table 1. Crystal structures, densities, and melting points of selected UHTCs.[20][21][22][23][24]

Material	Formula	Crystal structure	Lattice parameters (Å)			Density (g/cm^3)	Melting point	
			a	b	c		(°C)	(°F)
Hafnium carbide	HfC	FCC	4.638	4.638	4.638	12.76	3958	7156
Tantalum carbide	TaC	Cubic	4.455	4.455	4.455	14.50	3768	6814
Niobium carbide	NbC	Cubic	-	-	-	7.820	3490	-
Zirconium carbide	ZrC	Cubic	4.693	4.693	4.693	6.56	3400	6152
Hafnium nitride	HfN	FCC	4.525	4.525	4.525	13.9	3385	6125
Hafnium boride	HfB_2	Hexagonal	3.142	–	3.476	11.19	3380	6116
Zirconium boride	ZrB_2	Hexagonal	3.169	–	3.530	6.10	3245	5873
Titanium boride	TiB_2	Hexagonal	3.030	–	3.230	4.52	3225	5837
Titanium carbide	TiC	Cubic	4.327	4.327	4.327	4.94	3100	5612
Niobium boride	NbB_2	Hexagonal	3.085	-	3.311	6.97	3050	
Tantalum boride	TaB_2	Hexagonal	3.098	–	3.227	12.54	3040	5504
Titanium nitride	TiN	FCC	4.242	4.242	4.242	5.39	2950	5342
Zirconium nitride	ZrN	FCC	4.578	4.578	4.578	7.29	2950	5342
Silicon carbide	SiC	Polymorphic	–	Various	–	3.21	2545	4613
Vanadium carbide	VC	Cubic	-	-	-	5.77	2810 unstable	-

Tantalum nitride	TaN	Cubic	4.330	4.330	4.330	14.30	2700	4892
Niobium nitride	NbN	Cubic	-	-	-	8.470	2573	-
Vanadium nitride	VN	Cubic	-	-	-	6.13	2050 unstable ?	-

Structure

UHTCs all exhibit strong covalent bonding which gives them structural stability at high temperatures. Metal carbides are brittle due to the strong bonds that exist between carbon atoms. The largest class of carbides, including Hf, Zr, Ti and Ta carbides have high melting points due to covalent carbon networks although carbon vacancies often exist in these materials;[25] indeed, HfC has one of the highest melting points of any material. Nitrides such as ZrN and HfN have similarly strong covalent bonds but their refractory nature makes them especially difficult to synthesize and process. The stoichiometric nitrogen content can be varied in these complexes based on the synthetic technique utilized; different nitrogen content will give different properties to the material, such as how if x exceeds 1.2 in ZrNx, a new optically transparent and electrically insulating phase appears to form. Ceramic borides such as HfB_2 and ZrB_2 benefit from very strong bonding between boron atoms as well as strong metal to boron bonds; the hexagonal close-packed structure with alternating two-dimensional boron and metal sheets give these materials high but anisotropic strength as single crystals. Borides exhibit high thermal conductivity (on the order of 75–105 W/mK) and low coefficients of thermal expansion ($5–7.8 \times 10^{-6}\ K^{-1}$) and improved oxidation resistance in comparison to other classes of UHTCs. Thermal expansion, thermal conductivity and other data are shown in Table 2. The crystal structures, lattice parameters, densities, and melting points of different UHTCs are shown in Table 1.[11]

Table 2. Thermal expansion coefficients across selected temperature ranges and thermal conductivity at a fixed temperature for selected UHTCs.[13][26][27][28]

Material	Thermal expansion (10^{-6}/K)	Temp. range (°C)	Thermal cond. (W/mK)	Temperature (°C)
HfB_2–20%SiC			62	1000
ZrB_2–20%SiC	5–7.8	400–1600	78	1000
HfN	6.5	20–1000	22	800
HfC	6.6	20–1500	30	800
HfB_2	7.6	20–2205	70	800
TiB_2	8.6	20–2205		
ZrB_2	8.3	20–2205		
TaB_2	8.4	1027–2027	36.2	2027
ZrC	5.2	1027–2027		
TiC	7.7	20–1500		
TaC	6.3	20–1500		
SiC	1.1–5.5	20–1500	26.3	1500

Thermodynamic properties

In comparison with carbide and nitride-based ceramics, diboride-based UHTCs exhibit higher thermal conductivity (refer to Table 2, where we can see that hafnium diboride has thermal conductivity of 105, 75, 70 W/m*K at different temperature while hafnium carbide and nitride have values only around 20W/m*K).[29] Thermal shock resistance of HfB_2 and ZrB_2 was investigated by ManLabs and it was found that these materials did not fail at thermal gradients sufficient for the failure of SiC; indeed, it was found that hollow cylinders could not be cracked by an applied radial thermal gradient without first being notched on the inner surface. UHTCs generally exhibit thermal expansion coefficients in the range of 5.9–8.3 × 10^{-6} K^{-1}.The structural and thermal stability of ZrB_2 and HfB_2 UHTCs results from the occupancy of bonding and antibonding levels in hexagonal MB_2 structures with alternating hexagonal sheets of metal and boride atoms. In such structures, the principal frontier electronic states are bonding and antibonding orbitals resulting from bonding between boron 2p orbitals and metal d orbitals; before group (IV), the number of available electrons in a unit cell is insufficient to fill all bonding orbitals, and beyond it they begin to fill the antibonding orbitals. Both effects reduce the overall

bonding strength in the unit cell and therefore the enthalpy of formation and melting point. Experimental evidence shows that as one moves across the transition metal series in a given period, the enthalpy of formation of MB_2 ceramics increases and peaks at Ti, Zr, and Hf before decaying as the metal gets heavier. As a result, the enthalpies of formation of several important UHTCs are as follows: HfB_2 > TiB_2 > ZrB_2 > TaB_2 > NbB_2 > VB_2.[13]

Mechanical properties

Table 3 lists UHTC carbides and borides mechanical properties.[30] It is extremely important that UHTCs are able to retain high bending strength and hardness at high temperatures (above 2000 °C). UHTCs generally exhibit hardness above 20 GPa[31] due to the strong covalent bonds present in these materials. However, the different methods of processing UHTCs can lead to great variation in hardness values. UHTCs exhibit high flexural strengths of > 200 MPa at 1800 °C, and UHTCs with fine-grained particles exhibit higher flexural strengths than UHTCs with coarse grains. It has been shown that diboride ceramics synthesized as a composite with silicon carbide (SiC) exhibit increased fracture toughness (increase of 20% to 4.33 $MPam^{1/2}$) relative to the pure diborides. This is due to material densification[32] and a reduction in grain size upon processing.

Table. 3 Flexural strength, hardness, and Young's Modulus at given temperatures for selected UHTCs.[13][33][34][35]

The UHTC composites show higher mechanical properties like Tensile strength, Young's modulus, hardness, flexural strength, and fracture toughness at high temperatures as compared to monolithic UHTCs. The high sintering temperature and pressure result in high residual stress in the composites, which can be released at high temperatures. Therefore, the mechanical properties increase with the increase in temperature. [36][37][38][39][40][41][42][43]

At 1200°C the flexural strength of SiC is 170 MPa vs SiC-ZrC (10wt%) is 350Mpa. [40][39] **At 2000°C Titanium Carbide's flexural strength is 410 MPa vs TiC-WC(5%vol) is 491 MPa vs TiC-SiC(40%vol) is 543 Mpa.** [36][38] **Similarly the flexural strength for TaC-SiC(20%vol) is 715 Mpa at 1900°C which is about 40% higher than TaC (500 MPa) at the same temperature.**[43]

The Youngs modulus for TiC-WC(3.5wt%)-CNT(2wt%) at 1600°C is 428 GPa vs 300Gpa for TiC and the flexural toughness of TiC-WC(3.5wt%)-CNT(2wt%) at the same temperature is 8.1 MPa $m^{1/2}$ as compared to TiC which is 3.7 MPa $m^{1/2}$.[36][38] **For ZrC the fracture toughness at 1900°C is 4 MPa $m^{1/2}$ which increases to 5.8 MPa $m^{1/2}$ for ZrC-ZrO_2(40 wt.%).**[42]

The high strength of the materials is obtained due to the high homogeneities of the microstructures and the solute dispersion in the microstructures. [43][36][38][39]

A significant enhancement in hardness (~30%) of (Hf-Ta-Zr-Nb)C material compared to the monolithic UHTCs (HfC, TaC, ZrC, NbC) and in comparison to the hardest monocarbide (HfC) and the binary (Hf-Ta)C was recorded. The mechanism behind this enhancement in hardness maybe because of bonding behavior or some solid solution hardening effects arising from localized lattice strains. [37]

For applications based on combustion harsh environments and aerospace, Monolithic UHTCs are of concern because of their low fracture toughness and brittle behavior. UHTC composites are a potential approach to overcome these deficiencies. [44][45]

Material	Temperature(°C)	Young's Modulus(GPa)	Flexural Strength(MPa)	Hardness(GPa)
HfB_2	23	530	480	21.2–28.4
	800	485	570	
	1400	300	170	
	1800		280	
HfB_2–20%SiC	23	540	420	
	800	530	380	
	1400	410	180	
	1800		280	
ZrB_2	23	500	380	28.0
	800	480	430	
	1400	360	150	
	1800		200	
ZrB_2–20%SiC	23	540	400	
	800	500	450	
	1400	430	340	
	1800		270	
TaB_2	23	257		25.0
NbB_2	23	539		20.25
TiB_2	23	551	370	33.0
HfC	23	352		26.0
ZrC	23	348		27.0
TiC	23	451		30.0
TaC	23	285		18.2
SiC	23	415	359	32
	1000	392	397	8.9

Chemical properties

While UHTCs have desirable thermal and mechanical properties, they are susceptible to oxidation at their elevated operating temperatures. The metal component oxidizes to a gas such as CO_2 or NO_2, which is rapidly lost at the elevated temperatures UHTCs are most useful at; boron, for example, readily oxidizes to B_2O_3 which becomes a liquid at 490 °C and vaporizes very rapidly above 1100 °C; in addition, their brittleness makes them poor engineering materials. Current research targets increasing their toughness and oxidation resistance by exploring composites with silicon carbide, the incorporation of fibers, and the addition of rare-earth hexaborides such as lanthanum hexaboride (LaB_6). It has been found that the oxidative resistance of HfB_2 and ZrB_2 are greatly enhanced through the inclusion of 30% weight silicon carbide due to the formation of a protective glassy surface layer upon the application of temperatures in excess of 1000 °C composed of SiO_2.[46] To determine the effect of SiC content on diboride oxidation, ManLabs conducted a series of furnace oxidation experiments, in which the oxidation scale thickness as a function of temperature for pure HfB_2, SiC and HfB_2 20v% SiC were compared. At temperatures greater than 2100 K the oxide scale thickness on pure HfB_2 is thinner than that on pure SiC, and HfB_2/20% SiC has the best oxidation resistance. Extreme heat treatment leads to greater oxidation resistance as well as improved mechanical properties such as fracture resistance.[47]

Synthesis of diboride (Zr, Hf, Ti) UHTCs

UHTCs possess simple empirical formulas and thus can be prepared by a wide variety of synthetic methods. UHTCs such as ZrB_2 can be synthesized by stoichiometric reaction between constituent elements, in this case Zr and B. This reaction provides for precise stoichiometric control of the materials.[48] At 2000 K, the formation of ZrB_2 via stoichiometric reaction is thermodynamically favorable ($\Delta G = -279.6$ kJ mol^{-1}) and therefore, this route can be used to produce ZrB_2 by self-propagating high-temperature synthesis (SHS). This technique takes advantage of the high exothermic energy of the reaction to cause high temperature, fast combustion reactions. Advantages of SHS include higher purity of ceramic products, increased sinterability, and shorter processing times. However, the extremely rapid heating rates can result in incomplete reactions between Zr and B, the formation of stable oxides of Zr, and the retention of porosity. Stoichiometric reactions have also been carried out by reaction of attrition milled (wearing materials by grinding) Zr and B powder (and then hot pressing at 600 °C for 6 h), and nanoscale particles have been obtained by reacting attrition milled Zr and B precursor crystallites (10 nm in size).[49] Unfortunately, all of the stoichiometric reaction methods for

synthesizing UHTCs employ expensive charge materials, and therefore these methods are not useful for large-scale or industrial applications.

Reduction of ZrO_2 and HfO_2 to their respective diborides can also be achieved via metallothermic reduction. Inexpensive precursor materials are used and reacted according to the reaction below:

$$ZrO_2 + B_2O_3 + 5Mg \rightarrow ZrB_2 + 5MgO$$

Mg is used as a reactant in order to allow for acid leaching of unwanted oxide products. Stoichiometric excesses of Mg and B_2O_3 are often required during metallothermic reductions in order to consume all available ZrO_2. These reactions are exothermic and can be used to produce the diborides by SHS. Production of ZrB_2 from ZrO_2 via SHS often leads to incomplete conversion of reactants, and therefore double SHS (DSHS) has been employed by some researchers.[50] A second SHS reaction with Mg and H_3BO_3 as reactants along with the ZrB_2/ZrO_2 mixture yields increased conversion to the diboride, and particle sizes of 25–40 nm at 800 °C. After metallothermic reduction and DSHS reactions, MgO can be separated from ZrB_2 by mild acid leaching.

Synthesis of UHTCs by boron carbide reduction is one of the most popular methods for UHTC synthesis. The precursor materials for this reaction ($ZrO_2/TiO_2/HfO_2$ and B_4C) are less expensive than those required by the stoichiometric and borothermic reactions. ZrB_2 is prepared at greater than 1600 °C for at least 1 hour by the following reaction:

$$2ZrO_2 + B_4C + 3C \rightarrow 2ZrB_2 + 4CO$$

This method requires a slight excess of boron, as some boron is oxidized during boron carbide reduction. ZrC has also been observed as a product from the reaction, but if the reaction is carried out with 20–25% excess B_4C, the ZrC phase disappears, and only ZrB_2 remains.[32] Lower synthesis temperatures (~1600 °C) produce UHTCs that exhibit finer grain sizes and better sinterability. Boron carbide must be subjected to grinding prior to the boron carbide reduction in order to promote oxide reduction and diffusion processes.

Boron carbide reductions can also be carried out via reactive plasma spraying if a UHTC coating is desired. Precursor or powder particles react with plasma at high temperatures (6000–15000 °C) which greatly reduces the reaction time.[51] ZrB_2 and ZrO_2 phases have been formed using a plasma voltage and current of 50 V and 500 A, respectively. These coating materials exhibit uniform distribution of fine particles and porous microstructures, which increased hydrogen flow rates.

Another method for the synthesis of UHTCs is the borothermic reduction of ZrO_2, TiO_2, or HfO_2 with B.[52] At temperatures higher than 1600 °C, pure diborides can be obtained from this method. Due to the loss of some boron as boron oxide, excess boron is needed during borothermic reduction. Mechanical milling can lower the reaction temperature required during borothermic reduction. This is due to the increased particle mixing and lattice defects that result from decreased particle sizes of ZnO_2 and B after milling. This method is also not very useful for industrial applications due to the loss of expensive boron as boron oxide during the reaction.

Nanocrystals of group IV and V metal diborides such as TiB_2, ZrB_2, HfB_2, NbB_2, TaB_2 were successfully synthesized by Zoli's Reaction, reduction of TiO_2, ZrO_2, HfO_2, Nb_2BO_5, Ta_2O_5 with $NaBH_4$ using a molar ratio M:B of 1:4 at 700 °C for 30 min under argon flow.[53][54]

$MO_2 + 3NaBH_4 \rightarrow MB_2 + 2Na(g,l) + NaBO_2 + 6H_2(g)$ (M=Ti, Zr, Hf)

$M_2O_5 + 6.5NaBH_4 \rightarrow 2MB_2 + 4Na(g,l) + 2.5NaBO_2 + 13H_2(g)$ (M=Nb,Ta)

UHTCs can be prepared from solution-based synthesis methods as well, although few substantial studies have been conducted. Solution-based methods allow for low temperature synthesis of ultrafine UHTC powders. Yan et al. have synthesized ZrB_2 powders using the inorganic-organic precursors $ZrOC_{l2}$•$8H_2O$, boric acid and phenolic resin at 1500 °C.[55] The synthesized powders exhibit 200 nm crystallite size and low oxygen content (~ 1.0 wt%). UHTC preparation from polymeric precursors has also been recently investigated. ZrO_2 and HfO_2 can be dispersed in boron carbide polymeric precursors prior to reaction. Heating the reaction mixture to 1500 °C results in the in situ generation of boron carbide and carbon, and the reduction of ZrO_2 to ZrB_2 soon follows.[56] The polymer must be stable, processable, and contain boron and carbon in order to be useful for the reaction. Dinitrile polymers formed from the condensation of dinitrile with decaborane satisfy these criteria.

Chemical vapor deposition (CVD) of titanium and zirconium diborides is another method for preparing coatings of UHTCs. These techniques rely on metal halide and boron halide precursors (such as $TiCl_4$ and BCl_3) in the gaseous phase and use H2 as a reducing agent. This synthesis route can be employed at low temperatures and produces thin films for coating on metal (and other material) surfaces. Mojima et al. have used CVD to prepare coatings of ZrB_2 on Cu at 700–900 °C (Figure 2).[57] Plasma enhanced CVD (PECVD) has also been used to prepare UHTC diborides. After plasma of the reacting gases is created (by radio frequency or direct current discharge between two electrodes) the reaction takes place, followed by deposition. The deposition takes place at lower temperatures compared to traditional CVD because only the plasma needs to be heated to provide sufficient energy for the reaction. ZrB_2 has been prepared

via PECVD at temperatures lower than 600 °C as a coating on zircalloy.[58] Zirconium borohydride can also be used as a precursor in PECVD. Thermal decomposition of $Zr(BH)_4$ to ZrB_2 can occur at temperatures in the range of 150–400 °C in order to prepare amorphous, conductive films.[59]

Processing of UHTCs and the addition of SiC

Diboride-based UHTCs often require high-temperature and -pressure processing to produce dense, durable materials. The high melting points and strong covalent interactions present in UHTCs make it difficult to achieve uniform densification in these materials. Densification is only achieved at temperatures above 1800 °C once grain boundary diffusion mechanisms become active.[60] Unfortunately, processing of UHTCs at these temperatures results in materials with larger grain sizes and poor mechanical properties including reduced toughness and hardness. To achieve densification at lower temperatures, several techniques can be employed: additives such as SiC can be used in order to form a liquid phase at the sintering temperature, the surface oxide layer can be removed, or the defect concentration can be increased. SiC can react with the surface oxide layer in order to provide diboride surfaces with higher energy: adding 5–30 vol% SiC has demonstrated improved densification and oxidation resistance of UHTCs.[61] SiC can be added as a powder or a polymer to diboride UHTCs. The addition of SiC as a polymer has several advantages over the more traditional addition of SiC as a powder because SiC forms along the grain boundaries when added as a polymer, which increases measures of fracture toughness (by ~24%).[62] In addition to improved mechanical properties, less SiC needs to be added when using this method, which limits the pathways for oxygen to diffuse into the material and react. Although addition of additives such as SiC can improve densification of UHTC materials, these additives lower the maximum temperature at which UHTCs can operate due to the formation of eutectic liquids. The addition of SiC to ZrB_2 lowers the operating temperature of ZrB_2 from 3245 °C to 2270 °C.

Hot pressing is a popular method for obtaining densified UHTC materials that relies upon both high temperatures and pressures to produce densified materials. Powder compacts are heated externally and pressure is applied hydraulitically. In order to improve densification during hot pressing, diboride powders can undergo milling by attrition to obtain powders of <2μm. Milling also allows for more uniform dispersion of the additive SiC. Hot pressing temperature, pressure, heating rate, reaction atmosphere, and holding times are all factors that affect the density and microstructure of UHTC pellets obtained from this method. In order to achieve >99% densification from hot pressing, temperatures of 1800–2000 °C and pressures of 30 MPa or

greater are required. UHTC materials with 20vol.% SiC and toughened with 5% carbon black as additives exhibit increased densification above 1500 °C, but these materials still require temperatures of 1900 °C and a pressure of 30 MPa in order to obtain near theoretical densities.[63] Other additives such as Al_2O_3 and Y_2O_3 have also been used during the hot pressing of ZrB_2-SiC composites at 1800 °C.[64] These additives react with impurities to form a transient liquid phase and promote sintering of the diboride composites. The addition of rare earth oxides such as Y_2O_3, Yb_2O_3, La_2O_3 and Nd_2O_3 can lower densification temperatures and can react with surface oxides to promote densification.[65] Hot pressing may result in improved densities for UHTCs, but it is an expensive technique that relies on high temperatures and pressures to provide useful materials.

Pressureless sintering is another method for processing and densifying UHTCs. Pressureless sintering involves heating powdered materials in a mold in order to promote atomic diffusion and create a solid material. Compacts are prepared by uniaxial die compaction, and then the compacts are fired at chosen temperatures in a controlled atmosphere. Exaggerated grain growth that hinders densification occurs during sintering due to the low-intrinsic sinterability and the strong covalent bonds of Ti, Zr, and Hf diborides. Full densification of ZrB_2 by pressureless sintering is very difficult to obtain; Chamberlain et al. have only been able to obtain ~98% densification by heating at 2150 °C for 9 h (Figure 3).[66] Efforts to control grain size and improve densification have focused on adding third phases to the UHTCs, some examples of these phases include the addition of boron and iridium.[67] Addition of Ir in particular has shown an increase in the toughness of HfB_2/20vol.% SiC by 25%. Sintered density has also been shown to increase with the addition of Fe (up to 10% w/w) and Ni (up to 50% w/w) to achieve densifications of up to 88% at 1600 °C.[68] More advances in pressureless sintering must be made before it can be considered a viable method for UHTC processing.

Spark plasma sintering is another method for the processing of UHTC materials. Spark plasma sintering often relies on slightly lower temperatures and significantly reduced processing times compared to hot pressing. During spark plasma sintering, a pulsed direct current passes through graphite punch rods and dies with uniaxial pressure exerted on the sample material. Grain growth is suppressed by rapid heating over the range 1500–1900 °C; this minimizes the time the material has to coarsen. Higher densities, cleaner grain boundaries, and elimination of surface impurities can all be achieved with spark plasma sintering. Spark plasma sintering also uses a pulsed current to generate an electrical discharge that cleans surface oxides off of the powder. This enhances grain boundary diffusion and migration as well as densification of the material. The UHTC composite ZrB_2/20vol%SiC can be prepared with 99% density at 2000 °C in 5 min via spark plasma sintering.[69] ZrB2-SiC composites have also been prepared by spark plasma

sintering at 1400 °C over a period of 9 min.[70] Spark plasma sintering has proven to be a useful technique for the synthesis of UHTCs, especially for preparation of UHTCs with smaller grain sizes.

Applications

UHTCs, specifically Hf and Zr based diboride, are being developed to handle the forces and temperatures experienced by leading vehicle edges in atmospheric reentry and sustained hypersonic flight. The surfaces of hypersonic vehicles experience extreme temperatures in excess of 2500 °C while also being exposed to high-temperature, high-flow-rate oxidizing plasma. The material design challenges associated with developing such surfaces have so far limited the design of orbital re-entry bodies and hypersonic air-breathing vehicles such as scramjets and DARPA's HTV because the bow shock in front of a blunt body protects the underlying surface from the full thermal force of the onrushing plasma with a thick layer of relatively dense and cool plasma.

Sharp edges dramatically reduce drag, but the current generation of thermal protection system materials are unable to withstand the considerably higher forces and temperatures experienced by sharp leading edges in reentry conditions. The relation between radius of curvature and temperature in a leading edge is inversely proportional, i.e. as radius decreases temperature increases during hypersonic flight. Vehicles with "sharp" leading edges have significantly higher lift to drag ratios, enhancing the fuel efficiency of sustained flight vehicles such as DARPA's HTV-3 and the landing cross-range and operational flexibility of reusable orbital spaceplane concepts being developed such as the Reaction Engines Skylon and Boeing X-33.[71]

Zirconium diboride is used in many boiling water reactor fuel assemblies due to its refractory nature, corrosion resistance, high-neutron-absorption cross-section of 759 barns, and stoichiometric boron content. Boron acts as a "burnable" neutron absorber because its two isotopes, 10B and 11B, both transmute into stable nuclear reaction products upon neutron absorption (4He + 7Li and 12C, respectively) and therefore act as sacrificial materials which protect other components which become more radioactive with exposure to thermal neutrons. However, the boron in ZrB2|ZrB_2 must be enriched in 11B because the gaseous helium evolved by 10B strains the fuel pellet of UO_2 creates a gap between coating and fuel, and increases the fuel's centerline temperature; such cladding materials[72] have been used on the uranium oxide fuel pellets in Westinghouse AP-1000 nuclear reactors.[73] The high thermal neutron absorbance of boron also has the secondary effect of biasing the neutron spectrum to higher energies, so the fuel pellet retains more radioactive 239Pu at the end of a fuel cycle. In addition to this

deleterious effect of integrating a neutron absorber on the surface of a fuel pellet, boron coatings have the effect of creating a power density bulge in the middle of a nuclear reactor fuel cycle through the superposition of 235U depletion and faster burning of 11B. To help level out this bulge, ZrB_2/Gd cermets are being studied which would extend fuel lifetime by superimposing three simultaneous degradation curves.

Due to the combination of refractory properties, high thermal conductivity, and the advantages of large stoichiometric boron content outlined in the above discussion of integral neutron absorbing fuel pellet cladding, refractory diborides have been used as control rod materials and have been studied for use in space nuclear power applications.[74] While boron carbide is the most popular material for fast breeder reactors due to its lack of expense, extreme hardness comparable to diamond, and high cross-section, it completely disintegrates after a 5% burnup[75] and is reactive when in contact with refractory metals. Hafnium diboride also suffers from high susceptibility to material degradation with boron transmutation,[76] but its high melting point of 3380 °C and the large thermal neutron capture cross section of hafnium of 113 barns and low reactivity with refractory metals such as tungsten makes it an attractive control rod material when clad with a refractory metal.[77]

Titanium diboride is a popular material for handling molten aluminum due to its electrical conductivity, refractory properties, and its ability to wet with molten aluminum providing a superior electrical interface while not contaminating the aluminum with boron or titanium. TiB_2 has been used as a drained cathode in the electroreduction of molten Al(III). In drained-cathode processes, aluminum can be produced with an electrode gap of only 0.25m with an accompanying reduction in required voltage. However, implementation of such technology still faces hurdles: with a reduction in voltage, there is a concomitant reduction in heat generation and better insulation at the top of the reactor is required. In addition to improved insulation, the technology requires better bonding methods between TiB_2 and the bulk graphite electrode substrate. Bonding tiles of TiB_2 or applying composite coatings each present their own unique challenges, with the high cost and large TiB_2 capital cost of the former and the design difficulty of the latter. Composite materials must have each component degrade at the same rate, or the wettability and thermal conductivity of the surface will be lost with active material still remaining deeper within the electrode plate.[78]

ZrB_2/60%SiC composites have been used as novel conducting ceramic heaters which display high oxidation resistance and melting points, and do not display the negative temperature coefficient resistance property of pure silicon carbide. The metal-like conductance of ZrB_2 allows for its conductivity to decrease with increasing temperature, preventing uncontrollable

electrical discharge while maintaining high operational upper bounds for operation. It was also found that through incorporation of 40% ZrB_2 flexural strength was reduced from 500 MPa and 359 MPa in SiC and ZrB_2 single crystals to 212.96 MPa, with flexural strength highly correlated to the size of grains in the annealed ceramic material. Conductivity at 500 °C was found to be 0.005 Ω cm for the 40% SiC composite, versus 0.16 Ω cm in pure SiC.[79]

References

1. *Wuchina, E.; et al. (2007). "UHTCs: ultra-high temperature ceramic materials for extreme environment applications". The Electrochemical Society Interface. **16** (4): 30–36. doi:10.1149/2.F04074IF (https://doi.org/10.1149%2F2.F04074IF) .*
2. *Zhang, Guo-Jun; et al. (2009). "Ultrahigh temperature ceramics (UHTCs) based on ZrB2 and HfB2 systems: Powder synthesis, densification and mechanical properties" (https://doi.org/10.1088%2F1742-6596%2F176%2F1%2F012041) . Journal of Physics: Conference Series. **176** (1): 012041. Bibcode:2009JPhCS.176a2041Z (https://ui.adsabs.harvard.edu/abs/2009JPhCS.176a2041Z) . doi:10.1088/1742-6596/176/1/012041 (https://doi.org/10.1088%2F1742-6596%2F176%2F1%2F012041) .*
3. *Lawson, John W., Murray S. Daw, and Charles W. Bauschlicher (2011). "Lattice thermal conductivity of ultra high temperature ceramics ZrB2 and HfB2 from atomistic simulations". Journal of Applied Physics. **110** (8): 083507–083507–4. Bibcode:2011JAP...110h3507L (https://ui.adsabs.harvard.edu/abs/2011JAP...110h3507L) . doi:10.1063/1.3647754 (https://doi.org/10.1063%2F1.3647754) . hdl:2060/20110015597 (https://hdl.handle.net/2060%2F20110015597) .*
4. *Monteverde, Frédéric & Alida Bellosi (2004). "Efficacy of HfN as sintering aid in the manufacture of ultrahigh-temperature metal diborides-matrix ceramics". Journal of Materials Research. **19** (12): 3576–3585. Bibcode:2004JMatR..19.3576M (https://ui.adsabs.harvard.edu/abs/2004JMatR..19.3576M) . doi:10.1557/jmr.2004.0460 (https://doi.org/10.1557%2Fjmr.2004.0460) .*
5. *Zhao, Hailei; et al. (2007). "In situ synthesis mechanism of ZrB2-ZrN composite". Materials Science and Engineering: A. **452**: 130–134. doi:10.1016/j.msea.2006.10.094 (https://doi.org/10.1016%2Fj.msea.2006.10.094) .*
6. *Zhu, Chun-Cheng, Xing-Hong Zhang, and Xiao-Dong He. (2003). "Self-propagating High-temperature Synthesis of TiC-TiB2/Cu Ceramic-matrix Composite". Journal of Inorganic Materials. **4**: 026.*
7. *Chen.TJ (1981). "Fracture characteristic of ThO_2 ceramics at high-temperature". American Ceramic Society Bulletin. **60**: 923.*
8. *Curtis, C. E. & J. R. Johnson. (1957). "Properties of thorium oxide ceramics". Journal of the American Ceramic Society. **40** (2): 63–68. doi:10.1111/j.1151-2916.1957.tb12576.x (https://doi.org/10.1111%2Fj.1151-2916.1957.tb12576.x) .*

9. *Wang, Yiguang; et al. (2012). "Oxidation Behavior of ZrB2–SiC–TaC Ceramics". Journal of the American Ceramic Society.*
10. *Sannikova, S. N., T. A. Safronova, and E. S. Lukin. (2006). "The effect of a sintering method on the properties of high-temperature ceramics". Refractories and Industrial Ceramics. **47** (5): 299–301. doi:10.1007/s11148-006-0113-y (https://doi.org/10.1007%2Fs11148-006-0113-y) . S2CID 137075476 (https://api.semanticscholar.org/CorpusID:137075476) .*
11. *Bansal, Narottam P., ed. (2004). Handbook of Ceramic Composites. Springer. p. 192. Bibcode:2005hcc..book.....B (https://ui.adsabs.harvard.edu/abs/2005hcc..book.....B) .*
12. *Bansal, Narottam P., ed. (2004). Handbook of Ceramic Composites. Springer. p. 198. Bibcode:2005hcc..book.....B (https://ui.adsabs.harvard.edu/abs/2005hcc..book.....B) .*
13. *Sackheim, Robert L. (2006). "Overview of United States space propulsion technology and associated space transportation systems" (https://zenodo.org/record/1235935) . Journal of Propulsion and Power. **22**: 1310. doi:10.2514/1.23257 (https://doi.org/10.2514%2F1.23257) .*
14. *S. M. Johnson; Matt Gasch; J. W. Lawson; M. I. Gusman; M. M. Stackpole (2009). Recent Developments in Ultra High Temperature Ceramics at NASA Ames. 16th AIAA/DLR/DGLR International Space Planes and Hypersonic Systems and Technologies Conference.*
15. *Salute, Joan; et al. (2001). SHARP-B 2: Flight Test Objectives, Project Implementation and Initial Results. 2nd Annual Conference on Composites, Materials and Structures, Cocoa Beach, FL, United States. Vol. 22.*
16. *Shimada, Shiro. (2002). "A thermoanalytical study on the oxidation of ZrC and HfC powders with formation of carbon". Solid State Ionics. **149** (3–4): 319–326. doi:10.1016/s0167-2738(02)00180-7 (https://doi.org/10.1016%2Fs0167-2738%2802%2900180-7) .*
17. *Bargeron, C. B.; et al. (1993). "Oxidation Mechanisms of Hafnium Carbide and Hafnium Diboride in the Temperature Range 1400 to 21C". Johns Hopkins APL Technical Digest. **14**: 29–35.*
18. *Levine, Stanley R.; et al. (2002). "Evaluation of ultra-high temperature ceramics for aeropropulsion use". Journal of the European Ceramic Society. **22** (14–15): 2757–2767. doi:10.1016/s0955-2219(02)00140-1 (https://doi.org/10.1016%2Fs0955-2219%2802%2900140-1) .*
19. *Johnson, Sylvia (2011). Ultra High Temperature Ceramics: Application, Issues and Prospects. 2nd Ceramic Leadership Summit, Baltimore, MD.*
20. *Jenkins, R.; et al. (1988). "Powder Diffraction File: from the International Center for Diffraction Data". Swarthmore, PA.*
21. *Schwetz, K. A., Reinmoth, K. and Lipp (1981). "A. Production and Industrial Uses of Refractory Borides". Radex Rundschau: 568–585.*
22. *McColm, I.C. (1983). Ceramic Science for Materials Technologists. Chapman & Hall. pp. 330–343. ISBN 0412003511.*

23. *Pankratz, L. B., Stuve, J. M. and Gokcen, N. A. (1984). "Thermodynamic Data for Mineral Technology". Bulletin 677, U.S. Bureau of Mines: 98–102.*

24. *Cedillos-Barraza, Omar; Manara, Dario; Boboridis, K.; Watkins, Tyson; Grasso, Salvatore; Jayaseelan, Daniel D.; Konings, Rudy J. M.; Reece, Michael J.; Lee, William E. (2016). "Investigating the highest melting temperature materials: A laser melting study of the TaC-HFC system" (https://www.ncbi.nlm.nih.gov/pmc/articles/PMC5131352) . Scientific Reports. **6**: 37962. Bibcode:2016NatSR...637962C (https://ui.adsabs.harvard.edu/abs/2016NatSR...637962C) . doi:10.1038/srep37962 (https://doi.org/10.1038%2Fsrep37962) . PMC 5131352 (https://www.ncbi.nlm.nih.gov/pmc/articles/PMC5131352) . PMID 27905481 (https://pubmed.ncbi.nlm.nih.gov/27905481) .*

25. *Barraud, Elodie; et al. (2008). "Mechanically activated solid-state synthesis of hafnium carbide and hafnium nitride nanoparticles". Journal of Alloys and Compounds. **456** (1–2): 224–233. doi:10.1016/j.jallcom.2007.02.017 (https://doi.org/10.1016%2Fj.jallcom.2007.02.017) .*

26. *Samsonov, G. V. & Vinitskii, I. M. (1980). Handbook of Refractory Compounds. Plenum Press.*

27. *Opeka, M. M., Talmy, I. G., Wuchina, E. J., Zaykoski, J. A. and Causey, S. J. (1999). "Mechanical, Thermal and Oxidation Properties of Refractory Hafnium and Zirconium Compounds" (https://zenodo.org/record/1260159) . J. Eur. Ceram. Soc. **19** (13–14): 2405–2414. doi:10.1016/s0955-2219(99)00129-6 (https://doi.org/10.1016%2Fs0955-2219%2899%2900129-6) .*

28. *Samsonov, G. V. & Serebryakova, T. I. (1978). "Classification of Borides". Sov. Powder Metall. Met.Ceram. (English Translation). **17** (2): 116–120. doi:10.1007/bf00796340 (https://doi.org/10.1007%2Fbf00796340) . S2CID 137246182 (https://api.semanticscholar.org/CorpusID:137246182) .*

29. *Fahrenholtz, W. G.; et al. (2004). "Processing and characterization of ZrB 2-based ultra-high temperature monolithic and fibrous monolithic ceramics". Journal of Materials Science. **39** (19): 5951–5957. Bibcode:2004JMatS..39.5951F (https://ui.adsabs.harvard.edu/abs/2004JMatS..39.5951F) . doi:10.1023/b:jmsc.0000041691.41116.bf (https://doi.org/10.1023%2Fb%3Ajmsc.0000041691.41116.bf) . S2CID 135860255 (https://api.semanticscholar.org/CorpusID:135860255) .*

30. *Bansal, Narottam P., ed. (2004). Handbook of Ceramic Composites. Springer. p. 211. Bibcode:2005hcc..book.....B (https://ui.adsabs.harvard.edu/abs/2005hcc..book.....B) .*

31. *Rhodes, W. H., Clougherty, E. V. and Kalish, D. (1968). "Research and Development of Refractory Oxidation Resistant Diborides". Part II, AFML-TR-68-190, ManLabs Inc., Cambridge, MA. IV: Mechanical Properties.*

32. *Zhang, Guo-Jun; et al. (2009). "Ultrahigh temperature ceramics (UHTCs) based on ZrB2 and HfB2 systems: Powder synthesis, densification and mechanical properties" (https://doi.org/10.1088%2F1742-6596%2F176%2F1%2F012041) . Journal of Physics: Conference Series. **176** (1): 012041. Bibcode:2009JPhCS.176a2041Z (https://ui.adsabs.harvard.edu/abs/2009JPhCS.176a2041Z) . doi:10.1088/1742-6596/176/1/012041 (https://doi.org/10.1088%2F1742-6596%2F176%2F1%2F012041) .*

33. *Rhodes, W. H., Clougherty, E. V. and Kalish, D. (1970). "Research and Development of Refractory Oxidation Resistant Diborides". Mechanical Properties. Part II, Vol. IV.*

34. *Munro, R. G. (1997). "Material Properties of a Sintered alpha-SiC". Journal of Physical and Chemical Reference Data. **26** (5): 1195–1203. Bibcode:1997JPCRD..26.1195M (https://ui.adsabs.harvard.edu/abs/1997JPCRD..26.1195M) . doi:10.1063/1.556000 (https://doi.org/10.1063%2F1.556000) .*

35. *K. Sairam; J.K. Sonber; T.S.R.Ch. Murthy; C. Subramanian; R.K. Fotedar; R.C. Hubli. (2014). "Reaction spark plasma sintering of niobium diboride". International Journal of Refractory Metals and Hard Materials. **43**: 259–262. doi:10.1016/j.ijrmhm.2013.12.011 (https://doi.org/10.1016%2Fj.ijrmhm.2013.12.011) .*

36. *Fattahi, M.; Asl, M.S.; Delbari, S.A.; Namini, A.S.; Ahmadi, Z.; Mohammadi, M. Role of nano-WC addition on microstructural, mechanical and thermal characteristics of TiC-SiCw composites. Int. J. Refract. Met. Hard Mater. 2020, 90, 105248.*

37. *Castle, E., Csanádi, T., Grasso, S. et al. Processing and Properties of High-Entropy Ultra-High Temperature Carbides. Sci Rep 8, 8609 (2018). https://doi.org/10.1038/s41598-018-26827-1*

38. *Mao, H.; Shen, F.; Zhang, Y.; Wang, J.; Cui, K.; Wang, H.; Lv, T.; Fu, T.; Tan, T. Microstructure and Mechanical Properties of Carbide Reinforced TiC-Based Ultra-High Temperature Ceramics: A Review. Coatings 2021, 11, 1444. https:// doi.org/10.3390/coatings11121444*

39. *Jianjun Sha, Shouhao Wang, Jixiang Dai, Yufei Zu, Wenqiang Li, Ruyi Sha. High-temperature Mechanical Properties and Their Influence Mechanisms of ZrC-Modified C-SiC Ceramic Matrix Composites up to 1600 °C. Materials 2020, 13(7), 1581; https://doi.org/10.3390/ma13071581*

40. *Vinci A, Zoli L, Sciti D, et al. Mechanical behaviour of carbon fibre reinforced TaC/SiC and ZrC/SiC composites up to 2100 ℃. J Eur Ceram Soc 2019, 39: 780–787*

41. *Ni, D., Cheng, Y., Zhang, J. et al. Advances in ultra-high temperature ceramics, composites, and coatings. J Adv Ceram 11, 1–56 (2022). https://doi.org/10.1007/s40145-021-0550-6*

42. *Min-Haga, Eungi and William D. Scott. "Sintering and mechanical properties of ZrC-ZrO2 composites." Journal of Materials Science 23 (1988): 2865-2870*

43. *Liu, Han et al. "Microstructure and mechanical properties of the spark plasma sintered TaC/SiC composites: Effects of sintering temperatures." Journal of The European Ceramic Society 32 (2012): 3617-3625*

44. *Stanley R. Levine and Elizabeth J. OpilaGlenn Research Center, Cleveland, Ohio. Characterization of an Ultra-High Temperature Ceramic Composite. https://ntrs.nasa.gov/api/citations/20040074335/downloads/20040074335.pdf*

45. *Sciti, Diletta; Silvestroni, Laura; Monteverde, Frédéric; Vinci, Antonio; Zoli, Luca (2018-10-17). Advances in Applied Ceramics. 117 (sup1): s70–s75. doi:10.1080/17436753.2018.1509822. ISSN 1743-6753.*

46. *Paul, A.; et al. (2012). "UHTC composites for hypersonic applications". The American Ceramic Society Bulletin. **91**: 22–28.*

47. *Tului, Mario; et al. (2008). "Effects of heat treatments on oxidation resistance and mechanical properties of ultra high temperature ceramic coatings". Surface and Coatings Technology. **202** (18): 4394–4398. doi:10.1016/j.surfcoat.2008.04.015 (https://doi.org/10.1016%2Fj.surfcoat.2008.04.015)* .

48. *Çamurlu, H. Erdem & Filippo Maglia. (2009). "Preparation of nano-size ZrB_2 powder by self-propagating high-temperature synthesis". Journal of the European Ceramic Society. **29** (8): 1501–1506. doi:10.1016/j.jeurceramsoc.2008.09.006 (https://doi.org/10.1016%2Fj.jeurceramsoc.2008.09.006)* .

49. *Chamberlain, Adam L., William G. Fahrenholtz, and Gregory E. Hilmas. (2009). "Reactive hot pressing of zirconium diboride". Journal of the European Ceramic Society. **29** (16): 3401–3408. doi:10.1016/j.jeurceramsoc.2009.07.006 (https://doi.org/10.1016%2Fj.jeurceramsoc.2009.07.006)* .

50. *Nishiyama, Katsuhiro; et al. (2009). "Preparation of ultrafine boride powders by metallothermic reduction method" (https://doi.org/10.1088%2F1742-6596%2F176%2F1%2F012043) . Journal of Physics: Conference Series. **176** (1): 012043. Bibcode:2009JPhCS.176a2043N (https://ui.adsabs.harvard.edu/abs/2009JPhCS.176a2043N) . doi:10.1088/1742-6596/176/1/012043 (https://doi.org/10.1088%2F1742-6596%2F176%2F1%2F012043)* .

51. *Karuna Purnapu Rupa, P.; et al. (2010). "Microstructure and Phase Composition of Composite Coatings Formed by Plasma Spraying of ZrO_2 and B_4C Powders". Journal of Thermal Spray Technology. **19** (4): 816–823. Bibcode:2010JTST...19..816K (https://ui.adsabs.harvard.edu/abs/2010JTST...19..816K) . doi:10.1007/s11666-010-9479-y (https://doi.org/10.1007%2Fs11666-010-9479-y) . S2CID 136019792 (https://api.semanticscholar.org/CorpusID:136019792)* .

52. *Peshev, P. & G. Bliznakov. (1968). "On the borothermic preparation of titanium, zirconium and hafnium diborides". Journal of the Less Common Metals. **14**: 23–32. doi:10.1016/0022-5088(68)90199-9 (https://doi.org/10.1016%2F0022-5088%2868%2990199-9)* .

53. *Zoli, Luca; Costa, Anna Luisa; Sciti, Diletta (December 2015). "Synthesis of nanosized zirconium diboride powder via oxide-borohydride solid-state reaction". Scripta Materialia. **109**: 100–103. doi:10.1016/j.scriptamat.2015.07.029 (https://doi.org/10.1016%2Fj.scriptamat.2015.07.029)* .

54. *Zoli, Luca; Galizia, Pietro; Silvestroni, Laura; Sciti, Diletta (23 January 2018). "Synthesis of group IV and V metal diboride nanocrystals via borothermal reduction with sodium borohydride" (https://zenodo.org/record/1292491) . Journal of the American Ceramic Society. **101** (6): 2627–2637. doi:10.1111/jace.15401 (https://doi.org/10.1111%2Fjace.15401)* .

55. *Yan, Yongjie; et al. (2006). "New Route to Synthesize Ultra-Fine Zirconium Diboride Powders Using Inorganic–Organic Hybrid Precursors". Journal of the American Ceramic Society. **89** (11): 3585–3588. doi:10.1111/j.1551-2916.2006.01269.x (https://doi.org/10.1111%2Fj.1551-2916.2006.01269.x)* .

56. *Su, Kai & Larry G. Sneddon. (1993). "A polymer precursor route to metal borides". Chemistry of Materials. **5** (11): 1659–1668. doi:10.1021/cm00035a013 (https://doi.org/10.1021%2Fcm00035a013)* .

57. *Motojima, Seiji, Kimie Funahashi, and Kazuyuki Kurosawa. (1990). "ZrB_2 coated on copper plate by chemical vapour deposition, and its corrosion and oxidation stabilities". Thin Solid Films. **189** (1): 73–79. Bibcode:1990TSF...189...73M (https://ui.adsabs.harvard.edu/abs/1990TSF...189...73M) . doi:10.1016/0040-6090(90)90028-c (https://doi.org/10.1016%2F0040-6090%2890%2990028-c) .*

58. *Pierson, J. F.; et al. (2000). "Low temperature ZrB2 remote plasma enhanced chemical vapor deposition". Thin Solid Films. **359** (1): 68–76. Bibcode:2000TSF...359...68P (https://ui.adsabs.harvard.edu/abs/2000TSF...359...68P) . doi:10.1016/s0040-6090(99)00721-x (https://doi.org/10.1016%2Fs0040-6090%2899%2900721-x) .*

59. *Reich, Silvia; et al. (1992). "Deposition of thin films of Zirconium and Hafnium Boride by plasma enhanced chemical vapor deposition". Advanced Materials. **4** (10): 650–653. doi:10.1002/adma.19920041005 (https://doi.org/10.1002%2Fadma.19920041005) .*

60. *Sonber, J. K. & A. K. Suri. (2011). "Synthesis and consolidation of zirconium diboride: review". Advances in Applied Ceramics. **110** (6): 321–334. doi:10.1179/1743676111y.0000000008 (https://doi.org/10.1179%2F1743676111y.0000000008) . S2CID 136927764 (https://api.semanticscholar.org/CorpusID:136927764) .*

61. *Kaufman, Larry & Edward V. Clougherty. (1963). "Investigation of Boride Compounds for Very High-Temperature Applications". ManLabs. Inc., Cambridge, Mass.*

62. *Guron, Marta M., Myung Jong Kim, and Larry G. Sneddon. (2008). "A Simple Polymeric Precursor Strategy for the Syntheses of Complex Zirconium and Hafnium-Based Ultra High-Temperature Silicon-Carbide Composite Ceramics". Journal of the American Ceramic Society. **91** (5): 1412–1415. doi:10.1111/j.1551-2916.2007.02217.x (https://doi.org/10.1111%2Fj.1551-2916.2007.02217.x) .*

63. *Zhou, Shanbao; et al. (2010). "Microstructure, mechanical properties and thermal shock resistance of zirconium diboride containing silicon carbide ceramic toughened by carbon black". Materials Chemistry and Physics. **122** (2–3): 470–473. doi:10.1016/j.matchemphys.2010.03.028 (https://doi.org/10.1016%2Fj.matchemphys.2010.03.028) .*

64. *Zhu, Tao; et al. (2009). "Densification, microstructure and mechanical properties of ZrB_2–SiCw ceramic composites". Journal of the European Ceramic Society. **29** (13): 2893–2901. doi:10.1016/j.jeurceramsoc.2009.03.008 (https://doi.org/10.1016%2Fj.jeurceramsoc.2009.03.008) .*

65. *Zhang, Xinghong; et al. (2008). "Effects of Y2O3 on microstructure and mechanical properties of ZrB2-SiC ceramics". Journal of Alloys and Compounds. **465** (1–2): 506–511. doi:10.1016/j.jallcom.2007.10.137 (https://doi.org/10.1016%2Fj.jallcom.2007.10.137) .*

66. *Chamberlain, Adam L., William G. Fahrenholtz, and Gregory E. Hilmas. (2005). "Pressureless sintering of zirconium diboride". Journal of the American Ceramic Society. **89** (2): 450–456. doi:10.1111/j.1551-2916.2005.00739.x (https://doi.org/10.1111%2Fj.1551-2916.2005.00739.x) .*

67. *Wang, Xin-Gang, Wei-Ming Guo, and Guo-Jun Zhang. (2009). "Pressureless sintering mechanism and microstructure of ZrB_2–SiC ceramics doped with boron". Scripta Materialia. **61** (2): 177–180. doi:10.1016/j.scriptamat.2009.03.030 (https://doi.org/10.1016%2Fj.scriptamat.2009.03.030) .*

68. *Khanra, A. K. & M. M. Godkhindi. (2005). "Effect of Ni additives on pressureless sintering of SHS ZrB_2". Advances in Applied Ceramics. **104** (6): 273–276. doi:10.1179/174367606x69898 (https://doi.org/10.1179%2F174367606x69898) . S2CID 137453717 (https://api.semanticscholar.org/CorpusID:137453717) .*

69. *Venkateswaran, T.; et al. (2006). "Densification and properties of transition metal borides-based cermets via spark plasma sintering". Journal of the European Ceramic Society. **26** (13): 2431–2440. doi:10.1016/j.jeurceramsoc.2005.05.011 (https://doi.org/10.1016%2Fj.jeurceramsoc.2005.05.011) .*

70. *Zhao, Yuan; et al. (2009). "Effect of holding time and pressure on properties of ZrB_2-SiC composite fabricated by the spark plasma sintering reactive synthesis method". International Journal of Refractory Metals and Hard Materials. **27**: 177–180. doi:10.1016/j.ijrmhm.2008.02.003 (https://doi.org/10.1016%2Fj.ijrmhm.2008.02.003) .*

71. *J.F. Justin; A. Jankowiak (2011). "Ultra High Temperature Ceramics: Densification, Properties and Thermal Stability" (http://www.aerospacelab-journal.org/sites/www.aerospacelab-journal.org/files/AL3-08.pdf) (PDF). Journal AerospaceLab. 3, AL03-08.*

72. *Xu, Liang; et al. (2012). "Study on in-situ synthesis of ZrB2 whiskers in ZrB2 ZrC matrix powder for ceramic cutting tools". International Journal of Refractory Metals and Hard Materials.*

73. *Sironen, Charlton (2012). "Neutronic characteristics of using zirconium diboride and gadolinium in a Westinghouse 17x17 fuel assembly". University of South California, 1509920.*

74. *Sinclair, John (1974). "Compatibility of Refractory Materials for Nuclear Reactor Poison Control Systems". NASA Tm X-2963.*

75. *Sonber, J. K.; et al. (2010). "Investigations on synthesis of HfB_2 and development of a new composite with $TiSi_2$". International Journal of Refractory Metals and Hard Materials. **28** (2): 201–210. doi:10.1016/j.ijrmhm.2009.09.005 (https://doi.org/10.1016%2Fj.ijrmhm.2009.09.005) .*

76. *Ewing, Robert A. & Duane Neuman Sunderman. (1961). "Effects of Radiation Upon Hafnium Diboride".*

77. *Cheminant-Coatanlem, P.; et al. (1998). "Microstructure and nanohardness of hafnium diboride after ion irradiations". Journal of Nuclear Materials. **256** (2–3): 180–188. Bibcode:1998JNuM..256..180C (https://ui.adsabs.harvard.edu/abs/1998JNuM..256..180C) . doi:10.1016/s0022-3115(98)00059-2 (https://doi.org/10.1016%2Fs0022-3115%2898%2900059-2) .*

78. *Welch, Barry J (1999). "Aluminum production paths in the new millennium". Journal of the Minerals, Metals and Materials Society. **51** (5): 24–28. Bibcode:1999JOM....51e..24W (https://ui.adsabs.harvard.edu/abs/1999JOM....51e..24W) . doi:10.1007/s11837-999-0036-4 (https://doi.org/10.1007%2Fs11837-999-0036-4) . S2CID 110543047 (https://api.semanticscholar.org/CorpusID:110543047) .*

79. *Shin, Yong-Deok (2010). "The Development of an Electroconductive SiC-ZrB Composite through Spark Plasma Sintering under Argon Atmosphere" (https://doi.org/10.5370%2Fjeet.2010.5.2.342) . Journal of Electrical Engineering & Technology. **5** (2): 342–351. doi:10.5370/jeet.2010.5.2.342 (https://doi.org/10.5370%2Fjeet.2010.5.2.342) .*